PNNL-26474

Percheron Power – Small Business Vouchers Pilot Program Technology Assistance Report

Karri NK
Rakowski CL
Harding SF
Serkowski JA
Johnson KI
Richmond MC
Straalsund JL
Atkin SD
Hertelendy NZ

May 2017

Prepared for
the U.S. Department of Energy
under Contract DE-AC05-76RL01830

Pacific Northwest National Laboratory
Richland, Washington 99352

DISCLAIMER

PACIFIC NORTHWEST NATIONAL LABORATORY
operated by
BATTELLE
for the
UNITED STATES DEPARTMENT OF ENERGY
under Contract DE-AC05-76RL01830

Printed in the United States of America

Available to DOE and DOE contractors from the Office of Scientific and Technical Information,
P.O. Box 62, Oak Ridge, TN 37831-0062
www.osti.gov
ph: (865) 576-8401
fax: (865) 576-5728
email: reports@osti.gov

Available to the public from the National Technical Information Service
5301 Shawnee Rd., Alexandria, VA 22312
ph: (800) 553-NTIS (6847)
or (703) 605-6000
email: info@ntis.gov
Online ordering: http://www.ntis.gov

Summary

Battelle Memorial Institute, under U.S. Department of Energy Contract No. DE-AC05-76RL01830 to operate the Pacific Northwest National Laboratory (PNNL), agreed to provide technology assistance to Percheron Power in accordance with Small Business Vouchers Pilot Program Agreement project number 68798. This agreement was designed to provide assistance to Percheron Power in performing modeling and simulations for the design and optimization of composite Archimedes hydrodynamic screw (AHS) turbines.

This report documents the technical assistance provided to Percheron Power in developing, testing and manufacturing of composite AHS turbines. PNNL provided assistance mainly through computational modeling and physical-model testing support. The analysis documented in this report used advanced computational fluid dynamic (CFD) modeling to predict the performance of various turbine designs and parameters affecting their performance. The CFD analysis was later integrated with modern finite element analysis (FEA) to determine the optimal geometry and material requirements for specific turbine designs. Structural FEA was also conducted to address design and material-specific requirements such as blade root configuration, root anchoring requirements, cyclic loading potential, fiber orientation, and design-specific composite material mass. While the initial intent of this support was to develop an optimal composite AHS turbine design with strake-profiled blades for better performance, results from the modeling in conjunction with Percheron Power testing indicated that the a helicoid profile is cost - effective and preferable for the full-scale prototype testing when overall performance, material requirements, and the associated cost of manufacturing are considered.

Acknowledgments

The authors thanks the Small Business Vouchers Pilot program, an initiative of the U.S. Department of Energy's Office of Energy Efficiency & Renewable Energy, for supporting the work documented in this report.

Acronyms and Abbreviations

AHS	Archimedes Hydrodynamic Screw
CAD	Computer Aided Design
CFD	Computational Fluid Dynamics
DOE	U.S Department of Energy
DOF	Degrees of Freedom
EERE	Energy Efficiency and Renewable Energy
FEA	Finite Element Analysis
HBE	Helicoid Best Efficiency
HBV	Helicoid Best Volume
HRA	Hertelendy Research Associates Inc.
ID	Inside Diameter
kg	kilogram(s)
lb	pound(s)
LS	Load Step
m	meter(s)
m^3	cubic meter(s)
mm	millimeter(s)
MPa	megapascal(s)
OD	Outside Diameter
rpm	rotations per minute
SBE	Strake Best Efficiency
SBV	Strake Best Volume
UWRL	Utah Water Research Laboratory
VOF	Volume-of-Fluid
WSE	Water Surface Elevation

Contents

Figures

Tables

[redacted]

1.0 Introduction

Power generation using Archimedes Hydrodynamic Screw (AHS) turbines is a proven clean renewable energy technology for harnessing hydropower from low-head applications such as canals, river barriers, and diversion dams. Although AHS technology has been successfully deployed at a large scale in Europe where the cost of power generation is relatively high, the technology has not been adopted yet in the United States (U.S.), despite having huge potential to tap energy from low-head resources. Currently there are no AHS turbine manufacturers in the U.S. The main challenge for large-scale deployment of AHS technology in the U.S. is the levelized cost of energy. Present generation AHS steel turbines are expensive to manufacture and deploy because of the labor-intensive plate-forming, precision welding, and post-weld machining of the steel blades and central tubes, in addition to the transportation of large structures. Development of low-cost, modular AHS turbines with light-weight material such as composites may not only aid in widespread adoption of this technology, but also provides a competitive advantage for the manufacture of these turbines in the U.S.

This report documents the recent effort by Pacific Northwest National Laboratory (PNNL) in collaboration with Percheron Power, LLC, and Hertelendy Research Associates Inc.(HRA, Inc.) to design a potentially low-cost, light-weight glass-fiber composite AHS turbine using an integrated computational fluid dynamics (CFD) and structural analysis approach. The main focus of the work was to develop a low-cost structurally reliable turbine with optimal performance. Nevertheless, the nuances of turbine design with composite material instead of steel are also analyzed and discussed, as appropriate. The initial project intent was to develop and compare various optimized AHS turbine designs of composite material. Analytical models based on geometry optimization [1] and inflow conditions [2] indicate that there is an optimal fill volume that maximizes turbine performance. Recent studies [3] indicated that an AHS turbine with strake-profile blades may result in buckets having a greater volume than those of a helicoid screw having the same outer diameter, inclination, and number of blades. Moreover, such a gain in volume per turn and resulting performance is predicted to increase with the number of blades. However, results from the work presented in this report with integrated CFD and structural analysis of four-blade turbines indicated that the optimized helicoid profile is preferable to the strake profile when overall performance and associated costs of manufacturing are considered.

2.0 Project Scope

The scope of this project was to create free-surface CFD models of AHS turbine designs selected by Percheron Power for performance evaluations and perform integrated modeling with CFD and finite element analysis (FEA) for turbine design optimization. The objectives of the CFD analysis were to simulate performance by evaluating the hydrodynamic loading of the blades and to model various other parameters affecting efficiency, including bypass flow, friction forces, optimum orientation, etc. The CFD-generated hydrodynamic loading profiles were then input to the FEA for stress and deflection analysis. The goal was to use the model results with bench-scale testing to develop up to three prototype composite turbine designs using advanced manufacturing methods. One or more of these prototypes will then be water tested by Percheron Power at the Utah Water Research Laboratory (UWRL). The CFD analyses of the hydraulic performance were expected to provide critical insights to be applied when designing turbines with improved hydraulic efficiencies, particularly near the inlet and outlet regions. FEA was expected to optimize the turbine geometry for reduced weight, material requirements, and turbine cost. FEA was also expected to provide insights about blade connections to the central tube, blade root configuration, and loading requirements.

3.0 Approach

Integrated state-of-the-art CFD and FEA modeling techniques were coupled with flow experiments to develop and compare composite turbine designs with improved hydrodynamic and structural performance. The initial CFD models were validated simulating a bench-scale turbine that was built and tested by Percheron Power. CFD modeling was used later to estimate the performance of four prototype-scale turbine designs. Sensitivity studies were conducted with CFD to study the effect of gap leakage between the blades and the trough on performance, the effect of upstream and downstream water heads, and the effect of controlled rotation (constant rotational velocity). FEA modeling was used to estimate the stresses in the bench-scale and prototype-scale designs. The pressures obtained from the CFD models were mapped onto the FEA models for structural analyses. Initially, the bench-scale models were analyzed to establish a procedure for integrating the CFD-FEA analysis. The procedure was later followed to analyze the prototype-scale designs for static stresses at specific transient solutions (specific rotation rate) from the CFD. Structural FEA was performed to optimize the blade and tube thicknesses thereby estimating the material requirements for the four composite turbine designs considered. Design details related to blade root configuration, attachment bolt spacing, and overall turbine deflections were also addressed with FEA.

Two model scales were used in this work. The first set were reduced-scale (~1:10) models on which the bench-scale experiments were conducted. The computer aided design (CAD) models of the reduced-scale designs with details from the physical-model experiments were used to build the CFD models and the physical-model data were used to validate the CFD performance parameters such as torque, power output, efficiency, and discharge. The same CAD models, along with pressures mapped from CFD analysis, were used in FEA to streamline the procedure for detailed prototype-scale analysis. The details for how to later use approximate pressure profiles in FEA were established.

The second set of models included four different prototype-scale turbine designs for the best-efficiency and best-volume performance designs for the strake- and helicoid-shaped blades. For the initial turbine geometry, the blade and tube thicknesses were derived from existing literature about AHS steel turbine designs by accounting for the scaling in geometry and material strengths. Once the required dimensions were estimated, the CAD models of prototype designs developed by Percheron Power were used in the CFD analysis to estimate the performance. The pressures from the CFD analyses were used in the FEA for estimating the stresses and deflections in the blades and tube for the initial estimated geometry. The results from FEA provided initial under-design or over-design insights. Simplified shell models with average thicknesses from this second model set were later developed to estimate the optimal blade and tube thickness for different designs.

4.0 AHS Turbine Models for CFD and FEA

Four different turbine designs (Figure 1) were developed by Percheron Power for the optimized prototype comparisons. The designs included optimal efficiency and optimal volume turbines with helicoid- and strake-contoured blades. While the difference between helicoid and strake designs is the blade profile, the main differences between best-volume and best-efficiency designs are the blade pitch and the core tube diameter. The best-efficiency designs (Figure 1a and c) have smaller diameter tubes with longer blades and shorter blade pitch with a higher number of turns. All the prototype designs considered have the same blade outer diameter (OD) of 2 m and tube lengths of ~7.2 m. The blade inner diameter (ID; tube OD), thickness, span, and tube thickness (tube ID) vary for each design. Geometrical analysis indicated that the blade spans for strake models with blade angles of ~49° were approximately 32% longer than the

corresponding helicoid design spans. The initial estimates for the blade and tube thicknesses were obtained from scaling the literature requirements for AHS steel turbine design practices. For example, if the blade was approximated as a cantilever beam with pressure loading along the span, then the end deflection is proportional to kL^4/EI, where k is load constant, L is the length of the beam, E is modulus of elasticity, and I is the moment of inertia, which will be proportional to t^3, where 't' is the blade thickness.

For scaling based on the same end deflection for steel and composite blades of different lengths,

$$\frac{L_s^{\,4}}{E_s t_s^{\,3}} = \frac{L_c^{\,4}}{E_c t_c^{\,3}} \tag{1}$$

where subscript 's' denotes steel geometry and subscript 'c' denotes composite geometry. Therefore, the required composite blade thickness

$$t_c = t_s \left(\frac{L_c}{L_s} \right)^{4/3} \left(\frac{E_s}{E_c} \right)^{1/3} \tag{2}$$

Similarly, the bending deflection of a thin-walled tube supported at ends is proportional to

$$f(Length, Load) / EI \tag{3}$$

where 'I' is the moment of inertia, which will be proportional to R^3t, where 'R' is the pipe radius and 't' is the wall thickness (assuming thin wall). For the same deflection, and materials with different elastic properties, the product ER^3t will be the same and the required thickness for the composite tube is

$$t_c = t_s \left(\frac{E_s}{E_c} \right) \left(\frac{R_s}{R_c} \right)^3 \tag{4}$$

[redacted]

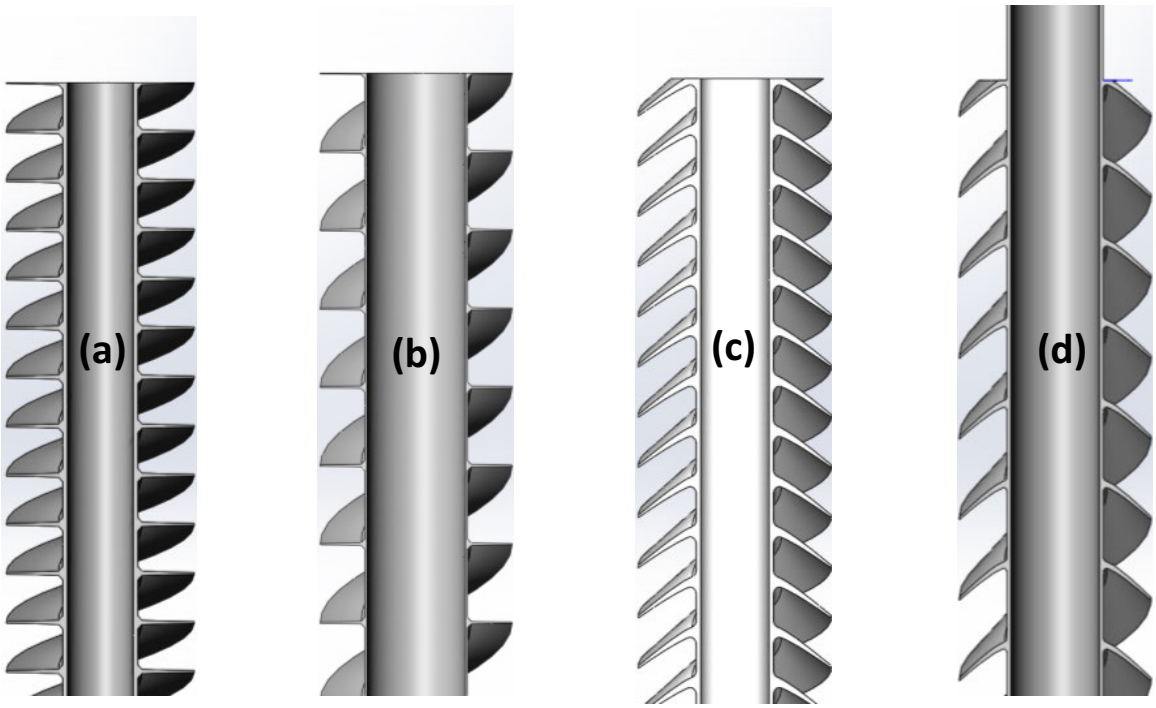

Figure 1. AHS turbine designs for the (a) Helicoid Best Efficiency (HBE), (b) Helicoid Best Volume (HBV), (c) Strake Best Efficiency (SBE), and (d) Strake Best Volume (SBV) models.

5.0 CFD Analyses for Turbine Performance and Parameter Sensitivity

A CFD model was used to simulate the flow through the AHS. A commercial CFD solver, STAR-CCM+, [4] was used to model the multi-phase (water and air) flow through the AHS designs provided by Percheron.

5.1 Geometry and Modeling Approach

CAD models for four prototype-scale and two reduced-scale AHS designs were provided by Percheron Power to PNNL. Best-volume and best-efficiency designs were supplied for a helicoid and a strake blade design for the prototype models. The "bench" model of a standard non-optimized helicoid design was modeled first (Figure 1). Note, the bench scale helicoid has different ID/OD and Pitch/OD ratios than the helicoid shown in Figure 1. This model included wide upstream and downstream boxes, and inlet and outlet boundaries that were the full water height. After visiting the physical-model bench scale test apparatus and observing test operations, it was noted that both the upstream and downstream boundaries were not the full height of the water depths, and that operating the AHS produced very strong recirculation in the downstream box. Downstream recirculation also occurred in the CFD model. The resulting inflow at the downstream boundary was undesirable. The CFD model was revised to reflect observed features and the inlet/outlet boxes for the prototype-scale designs were modified to improve behavior.

Each of the CAD geometries was subdivided into three regions (Figure 2) to facilitate their use in the CFD model. A cylindrical "moving region" was defined over the full length of the turbine blades to

accurately model the rotating screw. This rotating cylinder was enclosed in a thin "pipe" with the thickness of the tip gap between the screw blade and the trough (~2 mm, "gap region"). Meshing this tip gap separately increased the mesh quality, and hence solution quality, in this critical region. The remainder of the model included the upstream and downstream boxes, the downstream and upstream portions of the screw shaft not enclosed in the screw cylinder, and the air space above the screw and tip-gap region (the stationary region). The tip-gap region was well resolved with at least three cells in the gap and the mesh in the gap and moving regions were aligned with the axis of rotation to improve mesh quality. The models were composed of ~9.5M cells (helicoid models), 12.5 and 21M cells (SBV and SBE, respectively), and 26.8M cells (reduced-scale physical model). The CFD modeling in this work was performed using the PNNL Institutional Computing - Constance supercomputer.

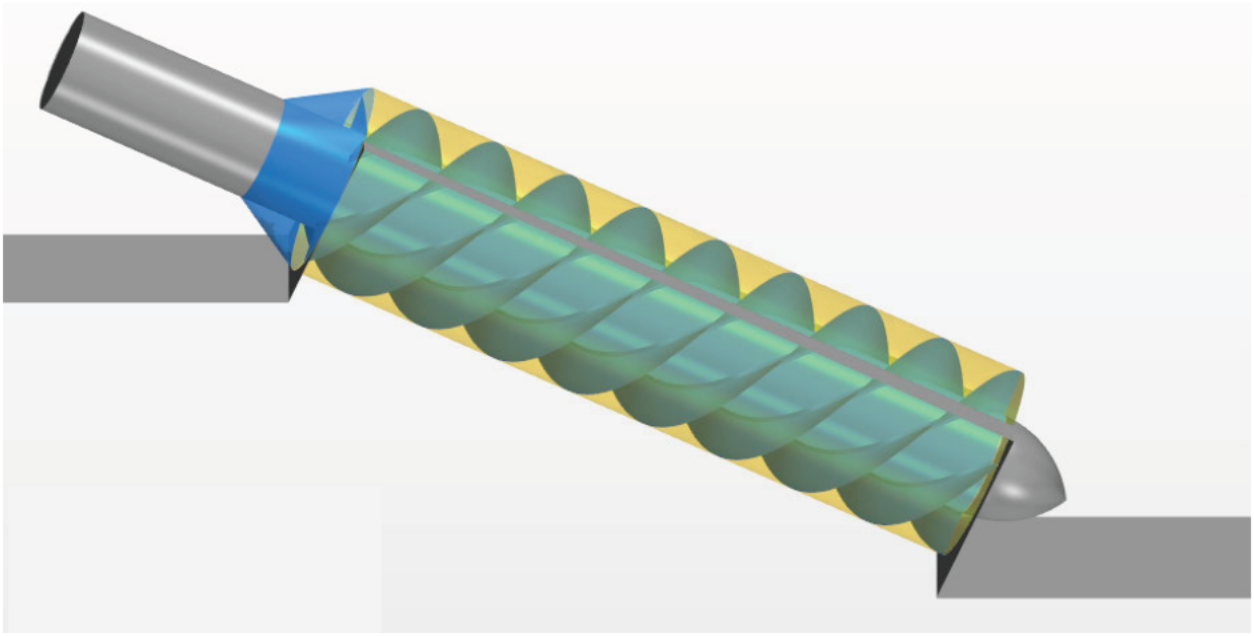

Figure 2. CFD geometry regions. Gold sleeve is the tip "gap" (which is the width of the gap between the blades and trough—2 mm and 0.4 mm in the prototype and bench models, respectively), the blue enclosing the blades is the moving region, and the rest (in gray) is the stationary region.

The flow domain was modeled using a transient, moving mesh, unsteady, volume-of-fluid (VOF) approach. The moving region had a specified rotation rate and sliding interfaces to the gap and stationary regions. The gap region (the "sleeve" encasing the moving section) had on its inner side an interface to the moving region. That interface had a majority of the area matched to the rotating mesh. The areas of the flat blade tips were assigned the specified rotational velocity of the blade tips. The exterior of the gap cylinder on the trough was specified as no-slip, the rest was a simple interface to the air of the stationary region. The stationary region contained the upstream and downstream hydrostatic boundaries of the specified water surface elevations. The rotational velocity of the screw was applied to the lengths of the screw shaft that were included in the stationary regions.

Boundary conditions were supplied by Percheron Power. The conditions modeled are listed in Table 1. Most of the prototype conditions were for the "overfill" condition specified by the water surface elevation in the head box. The HBV(heli_bv) geometry was run for additional boundary conditions: one with a slower rotation and one with lower water surface elevations in the upstream and downstream boxes. The angle of the prototype AHS was 25 degrees for all simulations. The bench model had two versions: with and without the tip gap; both had a fixed angle of 24.65 degrees.

Table 1. Designs and the boundary conditions modeled.

Design	Upper Box WSE (m)	Lower Box WSE (m)	head (m)	rpm
strake_be (SBE)	4.067	0.975	3.092	31.5
strake_bv (SBV)	4.017	0.988	3.029	31.5
heli_be (HBE)	4.067	0.975	3.092	31.5
heli_bv (HBV)	4.017	0.988	3.029	31.5
heli_bv_slow	4.017	0.988	3.029	26.0
heli_bv_levels	3.813	0.764	3.049	31.5
Bench - heli	0.516	0.181	0.335	94.2
Bench - nogap	0.516	0.181	0.335	94.2

WSE = water surface elevation.

The model physics included multi-phase flow of water and air using the VOF method. The simulations were transient (Δt = 0.00075 to 0.001 s), unsteady Reynold's-averaged Navier-Stokes, moving mesh simulations with a k-ε turbulence closure. Results included the calculation of torque and simulated flow, graphics, and movies of the transient results. The latter were used to improve understanding of the time-varying nature of the water level in the screw on the upstream side, the "signature" of the torque output, and the motion of the water within a given bucket, or "sloshing" within the screw.

5.2 CFD Validation

Using water surface elevations as the boundary conditions for the CFD model, the resulting simulated values of flow volume and torque were used as an independent check of model performance. Table 2 compares results from the CFD model and bench-scale tests. The bench-scale tests were run by setting the rotational rate and adjusting the flow rate to achieve the desired water surface elevations in the top and bottom boxes. The results reported were interpolated from the lab tests spanning the modeled conditions rather than exact match. In addition, the water surface within the "buckets" was compared to water testing of the reduced-scale physical model (Figure 3). The water surface plots were obtained by plotting the average surface levels within the buckets over a certain period. As shown in Figure 3, the CFD model accurately predicted the water fill level patterns evidenced in the physical experiment. The CFD model was also able to predict the two types of sloshing that occurred; one between adjacent blades and the other occurring periodically along the line of turbine blades.

Table 2. Comparison of the conventional (non-optimized) helicoid (with gap) bench-scale tests and CFD model results.

Performance Parameter	Experiment*	CFD Model	% Difference
Head (m)	0.387	0.335	13.44
Torque (N-m)	0.764	0.728	4.71
Flow rate (kg/s)	3.120	2.707	13.24
Efficiency	0.634	0.805	-26.97

*Experimental results correspond to the nearest experimental data point to the CFD boundary conditions, with the turbine speed matched at 94 rpm

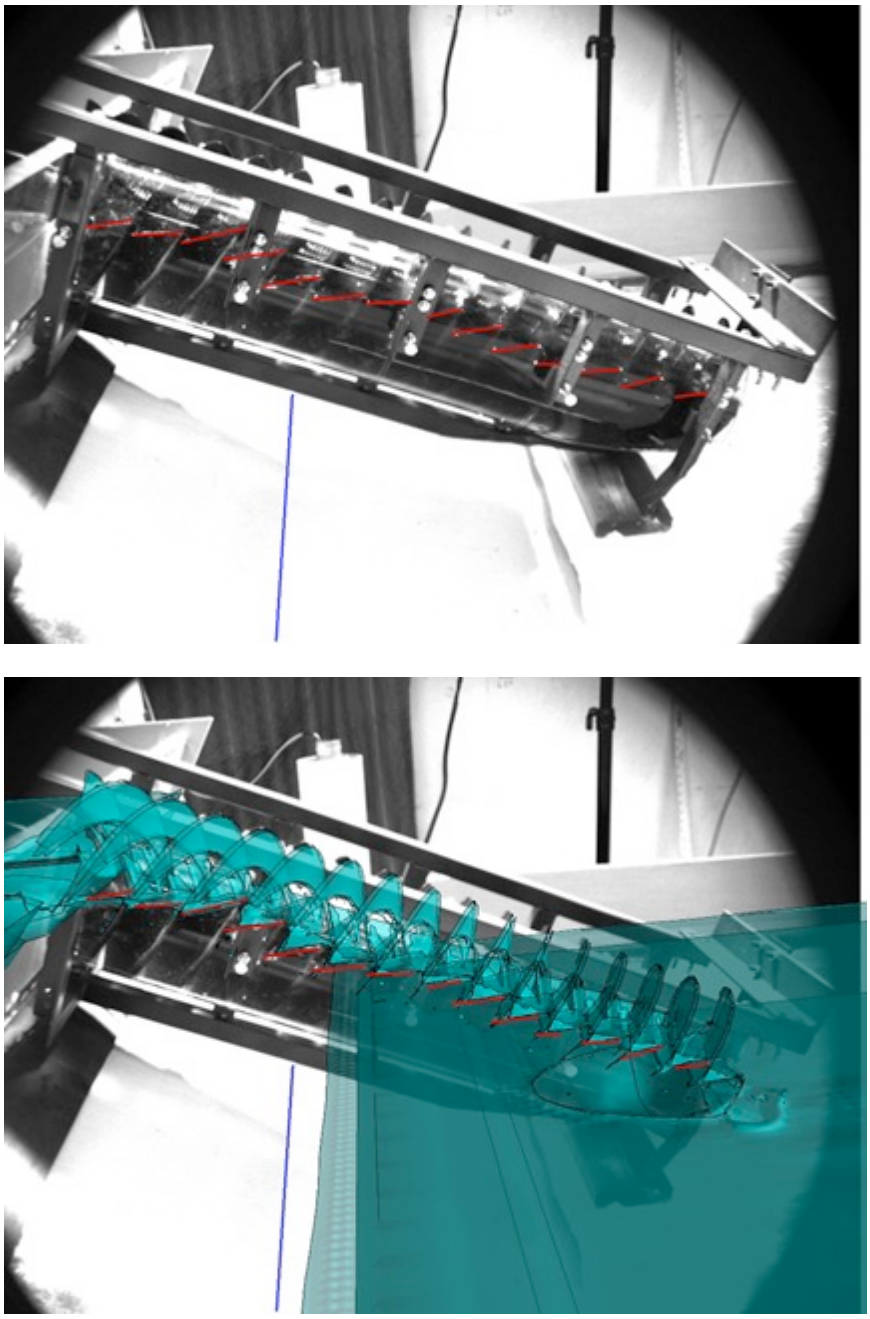

Figure 3. Comparison of water surface location for the conventional helicoid bench-scale turbine and the CFD model.

5.3 Results from CFD Analysis

After each of the simulations had run to a quasi-steady state, blade torque (moment) plots were created for several rotations of the screw (Figure 4–Figure 7). These plots show the periodic behavior of the torque (a function of rotation rate) and that the HBE design with the specified boundary conditions resulted in undesirable rapid changes in torque. Table 3 summarizes the torque and efficiencies from the eight designs and flows. Results from CFD analyses did not show the expected performance gain from strake designs. The results also indicated better torque efficiencies for helicoid designs. Note, however, that

these were run for overfill conditions as demonstrated in Figure 8 with the water flowing over the top of the screw at its downstream end.

A series of figures such as Figure 8 were used to visualize the flow results and movies were created to show the transient nature of the flows, within screw sloshing, interaction with tailrace waves, and bucket-fill patterns.

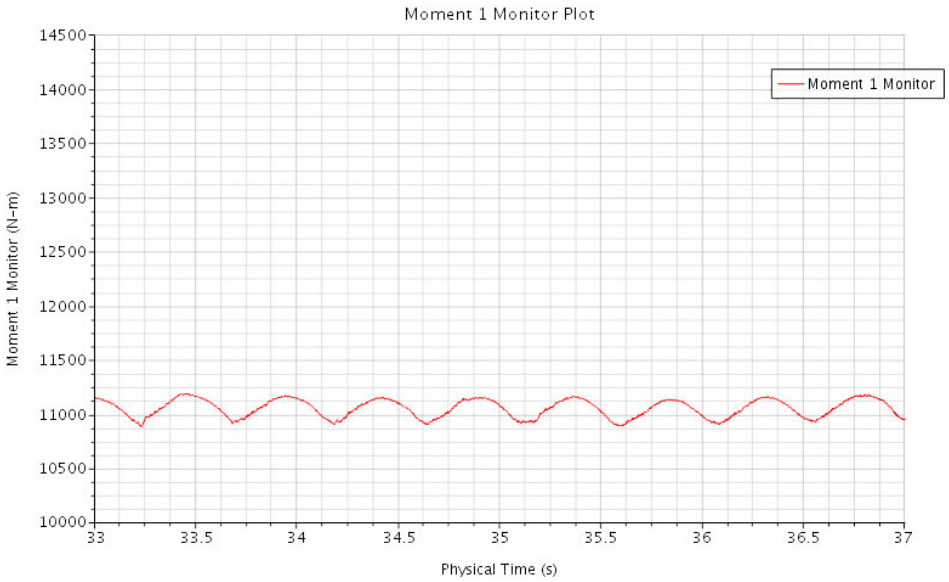

Figure 4. Time-history plot of torque from the SBE design.

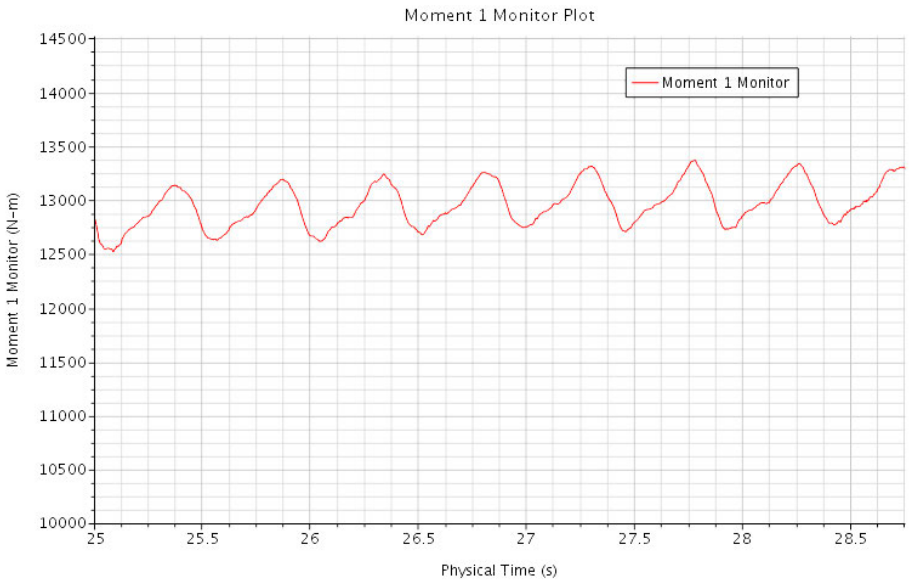

Figure 5. Time-history plot of torque from the HBV design.

[redacted]

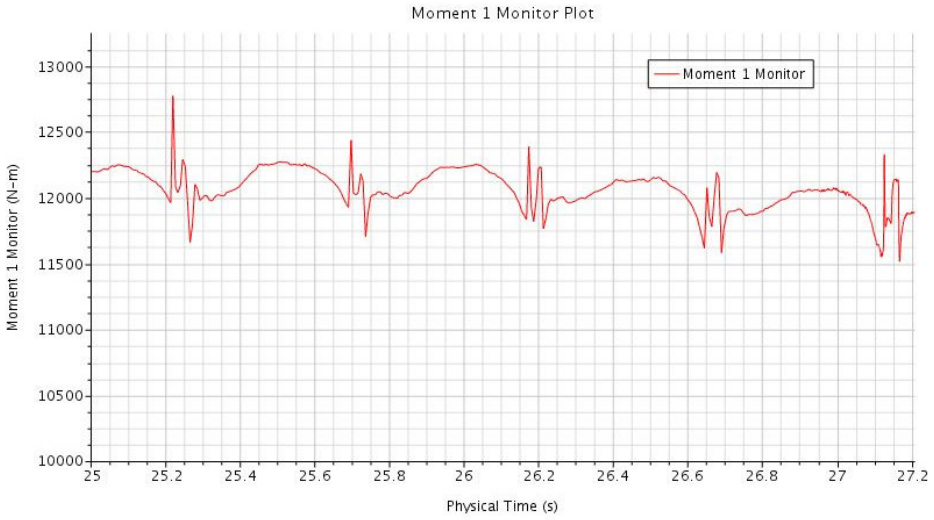

Figure 6. Time-history plot of torque from the HBE design.

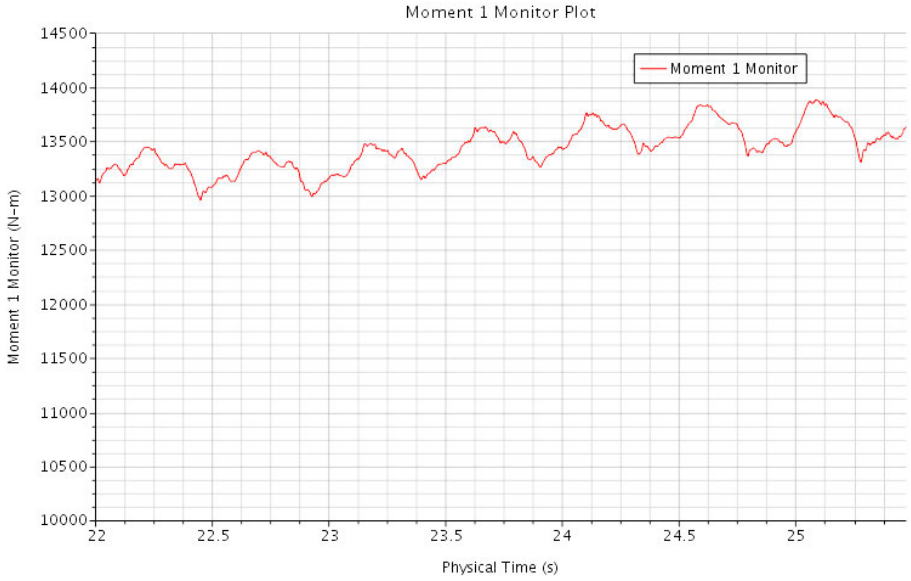

Figure 7. Time-history plot of torque from the SBV design.

Table 3. STAR-CCM+ results for torque and efficiency.

Design:	Torque(sim)	Q (kg/s)	Theoretical Torque	Torque Efficiency
strake_be	11041	1483	13623	0.810
strake_bv	12826	1873	16856	0.761
heli_be	11737	1400	12858	0.913
heli_bv	13614	1908	17170	0.793
heli_bv_slow	14500	1594	17383	0.834
heli_bv_levels	9838	1266	11464	0.858
Bench - heli	0.7279	2.717	0.90	0.805
Bench - nogap	0.7225	2.723	0.91	0.797

[redacted]

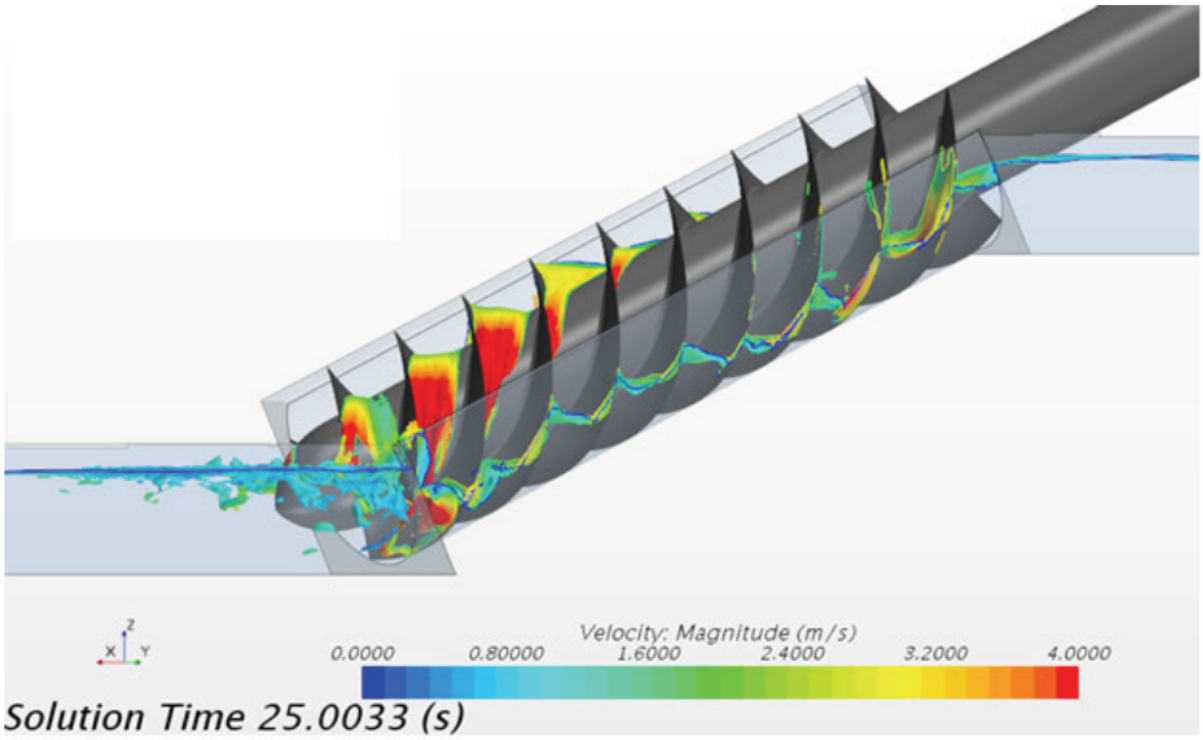

Figure 8. Simulated water surface and velocity within the AHS channel.

6.0 Pressure Mapping from CFD to FEA

The commercial FEA software ANSYS®[5] was used for all the structural analyses. The pressures on the blades and tube for FEA of the initial bench-scale and prototype-scale designs were obtained using CFD analysis. While the computational meshes for both the fluid dynamic analysis with STAR-CCM+ and the structural analysis with ANSYS were built from the same CAD files, the meshes differ significantly. Initially, the transient turbine models were solved in STAR-CCM+ using a finite volume mesh. Although the boundary conditions are unchanging, the flow solution changes with time because the turbine rotates. Once the CFD analysis was run to a quasi-static state, the surface pressures from a single point in time were applied to the ANSYS structural mesh for static load case analysis using the ANSYS solver. To map the pressures from CFD to FEA, the ANSYS FEA mesh was exported in the STAR-CCM+ readable *.cdb format that contained all the nodes and element nodal connectivity. The ANSYS mesh was imported into STAR-CCM+ and then rotated to coincide with the CFD mesh (element surfaces). Once the mesh was rotated to the proper orientation, the pressures from CFD model element faces were interpolated onto the finite element faces and exported. The export generated a text file macro (*.mac) that could be read directly in ANSYS to apply the CFD simulated pressure loads in the FEA.

7.0 Structural FEA for Turbine Design and Optimization

The ANSYS commercial FEA software was used to compute stresses and deflections in the composite turbine components. Models simulating the detailed prototype designs and simplified geometries were developed to optimize the turbine design. FEA was also used to analyze blade root configuration, blade connection to the tube, bolt spacing, etc.

7.1 Composite Property Estimation and Validation

The composite material properties required for the structural analysis were estimated using classical lamination theory. Initially, the composite properties were estimated based on the fiber and matrix properties, fiber volume fraction, orientation, and layup used in the prototype cantilever geometry tested by the blade fabricator (HRA Inc.). The cantilever test prototype used a layup of [0/45/-45] E-glass-fiber mat and an epoxy resin system with a fiber volume fraction of ~56.5% in the final composite. The glass-fiber volume fraction (56.5%) was calculated from the weight fractions of the HRA Inc cantilever test prototype. The composite properties estimated with classical lamination theory were used in the FEA model of the test prototype. The FEA model was constructed in ANSYS with two-dimensional plane strain elements. The deflections from the FEA were validated against test results and manual calculations.

Figure 9 presents the details of the prototype test geometry used by HRA Inc for the cantilever beam deflection test. As shown in the figure, the prototype has an 18" span, ¾"thickness, 3" width, and it includes 3/8" thick webs at the root. The base of the beam was about 0.7" thick. The beam was fixed to a rigid frame using a bolt that passes through a 300 series stainless steel plate of 2" × 1¼" × 0.5" (thickness) embedded in the base of the plate. A load of 46.6 lb was applied at a section 16" from the base. The beam deflection was measured at a location 5/8" from the free end.

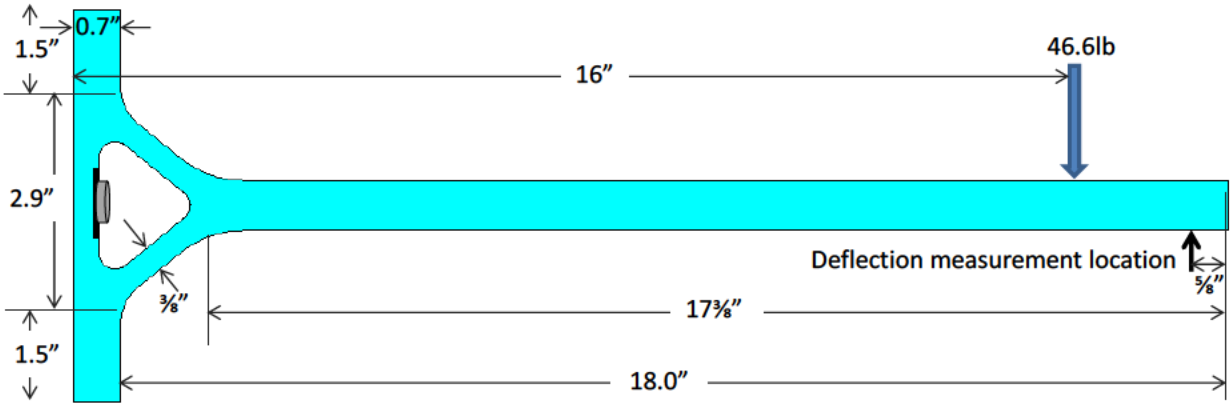

Figure 9. Composite cantilever geometry used for deflection test by HRA Inc.

The specific fiber and matrix materials used in the cantilever prototype are as follows:

- Fiber: SAERTEX [6] fabric with [0/45/-45] layup and areal-weight 1217 g/m^2
- Matrix: Rhino1401-21 / 4101-21 Epoxy resin system 7
- 24 layers in the span, 12 layers in the base.

The test produced a pre-fatigue deflection of 0.187" (4.75 mm) at 5/8" from the free end that compares well with the theoretical calculation result of 4.71 mm using the cantilever beam slope and deflection deflection equations (5) and (6), (δ=-W/6EI where W is the load applied at a distance 'a' from the free end, l is the span,, E is Young's modulus, and I is the cross-sectional area moment of inertia about the neutral axis).

$$y = -\frac{W}{6EI}(2l^3 - 3l^2a + a^3) \tag{5}$$

$$\theta = W\frac{(l-a)^2}{2EI} \tag{6}$$

Figure 10 shows the FEA results. The FEA simulation predicted a vertical deflection of 3.9 mm for a root with webs (Figure 10a) and similar to the test prototype, and 4.9 mm without the root (Figure 10b) in the model. These FEA results were in good agreement with the physical testing by HRA Inc. The slightly lower deflection from the FEA model of the actual geometry could be attributed to the homogeneous material properties used for the plane strain elements. Slip of the bolted joint in the lab tests may also add to the measured deflection of the composite laminate beam.

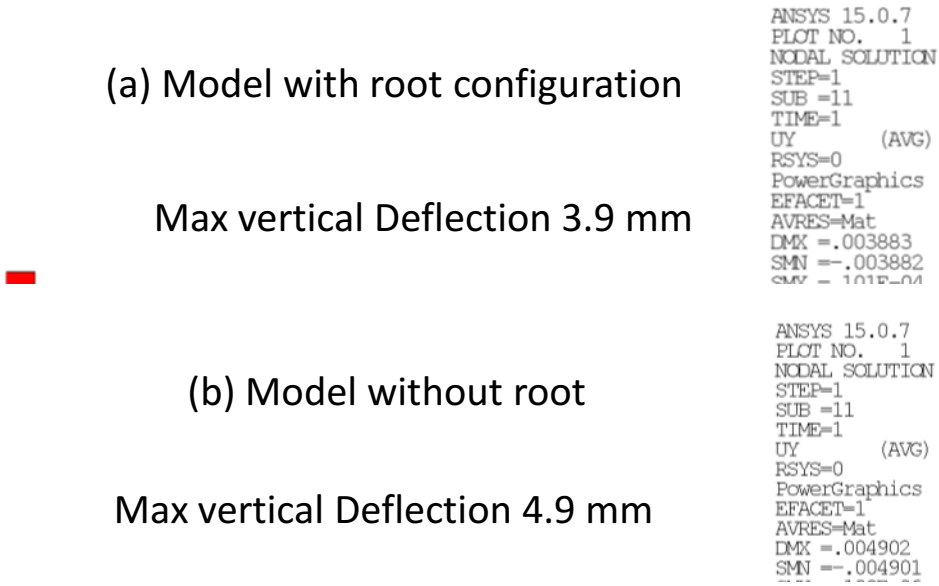

Figure 10. Deflection results (in m) from the FEA models with (a) and without (b) a root.

The estimated composite material properties were validated with the [0/+45/-45] fabricated layup. However, the quasi-isotropic [0/+45/-45/90] layup was recommended for the prototype development to eliminate the directional dependence of composite properties around the curving blades. This layup may reduce labor time during manufacturing because the quasi-isotropic mats can be placed in any orientation without consideration for loading direction, which otherwise be needed during layup of the mats with [0/+45/-45] orientations. Table 4 lists the calculated composite properties from the cantilever prototype and the recommended layups.

Table 4. Summary of calculated composite properties for the prototype and recommended layups.[(a)]

Property	Prototype Layup [0/45/-45]	Quasi-Isotropic [0/45/-45/90]
E_L (GPa)	22.26	21.58
E_T (GPa)	12.86	21.58
G_{LT} (GPa)	9.20	8.26
ν_{LT}	0.539	0.306
ν_{TL}	0.312	0.306

(a) Properties based on the following E-Glass and Epoxy properties

- E_f = 73.084 Gpa , G_f = 30.13 Gpa , ν_f = 0.22 , 60% fiber VF.
- E_m = 3 Gpa , G_m = 1.11 Gpa , ν_m=0.35, Rhino Epoxy resin system.

For the quasi-isotropic layup, the density of the composite was estimated based on 60% fiber volume fraction with glass-fiber and matrix densities of 2491 kg/m^3 and 1218 kg/m^3, respectively. The composite density used in the FEA models is 2491.2*0.6+1218*(1-0.6) = 1982 kg/m^3.

7.2 Structural Analysis of Prototype Geometries

Structural analysis of the initial prototype geometries based on scaling from the steel turbine design practices was performed to determine if such estimates result in a conservative or sub-optimum design. The initial prototype CAD models built in Solidworks by Percheron Power were exported in a parasolid binary (*.x_b) format for use in the FEA analysis with ANSYS. The models were meshed with ANSYS SOLID186 elements, the higher order three-dimensional 20-node solid element that exhibits quadratic displacement behavior. The FEA models had 128,000 elements (240,000 nodes, 0.72M DOF) for the HBE mesh, 160,000 elements (303,000 nodes, ~0.9M DOF) for the HBV mesh, 135,000 elements (250,000 nodes, 0.75M DOF) for the SBV mesh, and 283,000 elements (495,000 nodes, 1.5M DOF) for the SBE mesh.

The models were assigned with homogeneous material properties estimated for the quasi-isotropic layup discussed in Section 7.1. The end nodes at the periphery of the tube ID were fixed in the axial, radial, and circumferential directions for the boundary conditions. The FEA models were solved in three load steps (LS) that include 1) gravity, 2) gravity + pressure, and 3) gravity + pressure + rotation. The pressure loading for the second LS was obtained from the CFD models as discussed in Section 6.0. The pressure loads acting on the turbine at a point in time from the transient CFD solution were picked such that they correspond to a maximum torque point. Figure 11 illustrates the pressures loads mapped on the HBE and the SBE FEA models along with the gravity and angular rotation directions. A turbine rotation speed of 50 rpm was specified to capture the effect of rotational inertial loads on the blade deflections and stresses.

Figure 12a presents the total displacement and Figure 12b presents the maximum principal stress results from all three load steps of the HBE model. The results showed that the maximum deflections and stresses occurred on the blades with highest fill levels. The maximum tensile stresses occurred on the water-facing side of the blades toward the roots at the bottom of the tube. The maximum compressive stresses appeared on the back side of the blades toward the roots at the top of the tube. The stress results showed that the maximum tensile stresses were all less than 2 MPa. This value was well within the quasi-isotropic layup longitudinal and transverse strength of 236 MPa. This result indicated that the blade and tube thicknesses may be limited by deflection criteria rather than strength. The results from LS3 with rotational velocity in addition to gravity and pressure loads indicated little effect of the rotation inertial loads on the displacements and stresses in the turbine. Similar results were obtained from other designs.

Table 5 presents the summary of calculated torques from the FEA and CFD models. The agreement between the CFD and FEA analyses indicates proper transfer of loads with sufficient mesh resolution.

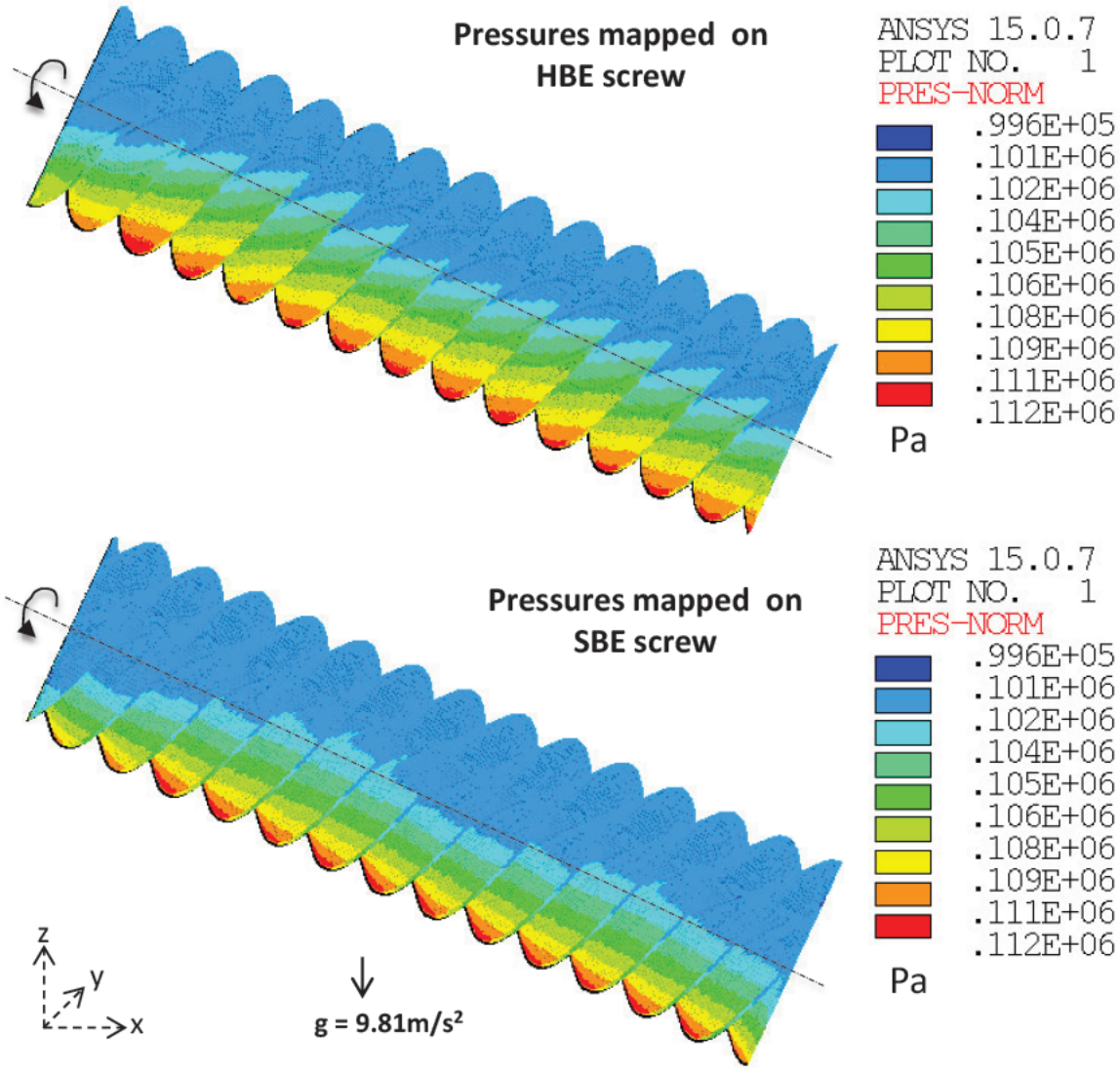

Figure 11. FEA models of the HBE and SBE turbine designs showing applied loads in the model.

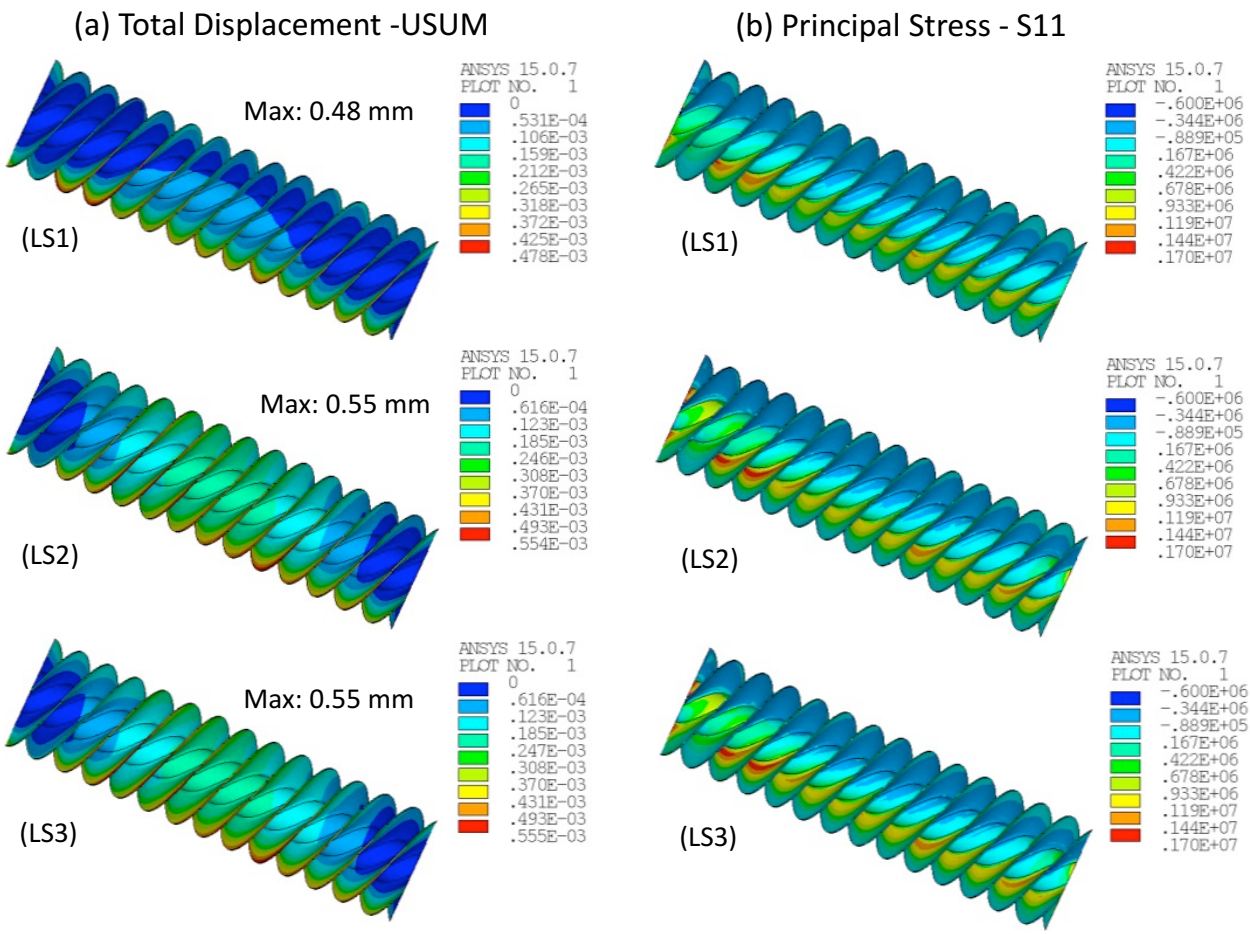

Figure 12. Displacements (in m) and maximum principal stresses (in Pa) from the three load steps of the HBE model.

Table 5. Summary of torques and total displacements from FEA.

FEA / CFD Model	Torque FEA (N-m)	Torque CFD (N-m)	U-Sum (mm)
HBE	11981	11900	0.55
HBV	13973	13750	1.60
SBE	11458	11175	0.96
SBV	13722	13400	0.80

NOTES:

- The FEA and CFD models were based on the CAD models provided by Percheron Power.
- Both the tube and blade materials were assumed to be the same.
- Blade and tube material properties were based on ~60% E-glass by volume (Quasi-Isotropic layup).
- U-Sum was the maximum of the net deflections from all the load steps.

7.3 Single-Flight Shell Element Models for Tube and Blade Thickness Estimation

The integrated CFD-FEA discussed earlier resulted in overly conservative designs. These analyses were based on prototype turbine geometry scaled from steel turbine design practices. Optimizing turbine geometries based on such analysis requires many iterations, which were not be feasible within the time and budget constraints of this project. To simplify and expedite the optimization process, single-flight shell element models were developed. These models represent a 360-degree repeating unit from each of the four designs considered in this work. The blade angles for the strake and helicoid models were obtained from the midline measurements of the corresponding CAD models. The shell models were constructed with uniform blade thickness to estimate the upper bound composite volume. Tapered blades may reduce the blade volume for similar deflections. The blades in shell models were not continuous and were disconnected at the 180-degree location to represent the 180-degree modular blade sections expected in the prototypes. Having disconnected flights in these models captures maximum deflections that may occur in prototypes when one 180-degree flight is completely under water. Figure 13 shows the single-flight shell model of the HBE design with pressure loads.

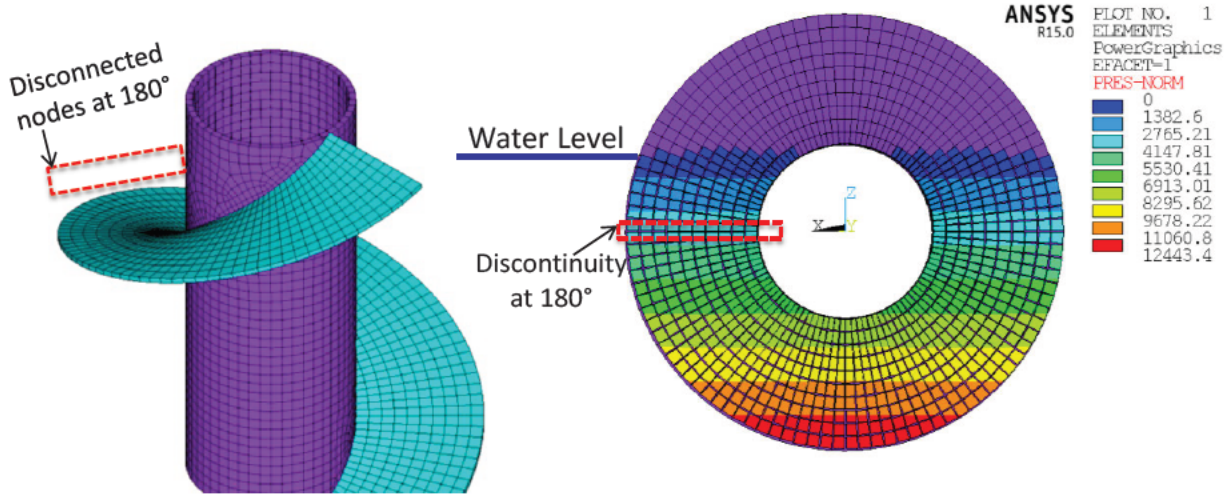

Figure 13. Single-flight HBE shell model with applied pressure load (Pa).

The pressure loads on the shell models were applied such that one 180-degree section is completely immersed in water. The pressures applied to the simplified shell models followed the hydrostatic approximation ("ρgh" variation in the direction of gravity accounting for tube inclination) based on the bounding profile derived from the CFD mapped pressures. Figure 14a presents the pressure variation with depth along the periphery of a SBE screw blade along with the pressure head "ρgh" variation (Figure 14b). As shown in this figure, the "ρgh" variation conservatively bounds the front side pressures. The integrated CFD-FEA approach discussed in earlier sections captures the real world loads where the net load on the blades is the difference between the front and backside pressures that will be well below the "ρgh" variation used in the simplified models.

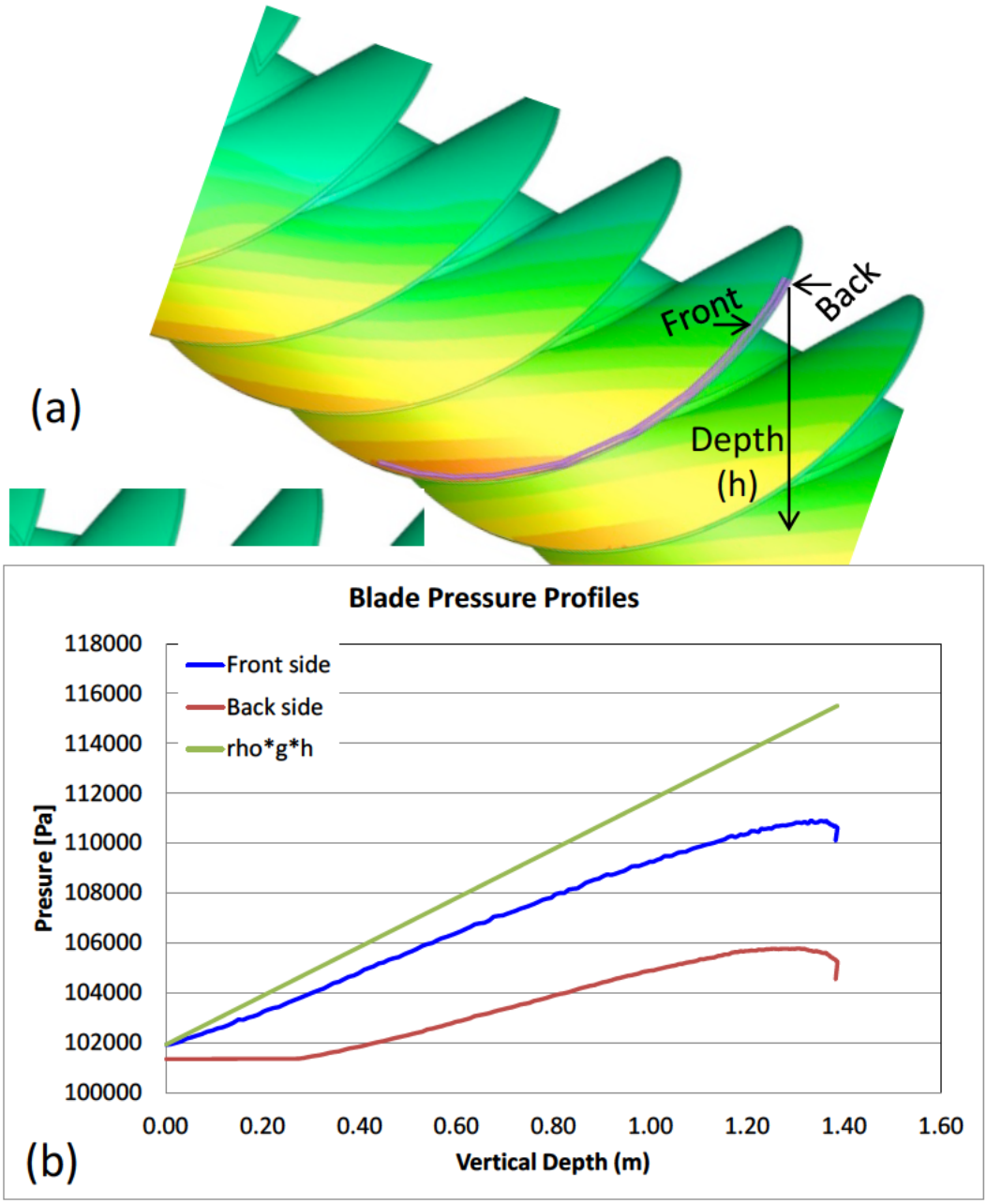

Figure 14. Pressure load variation on the front and back sides near the periphery of the SBE blade (a) compared to the hydrostatic (ρgh) variation (b).

The blades in the single-flight shell models used the quasi-isotropic layup [0/45/-45/90] composite properties listed in Table 4. The tube was assigned with the published composite properties of Ershigs® 55° helical wound pressure pipe [8]. For boundary conditions, the nodes on one end of the tube were constrained in all directions to represent the tube end condition and the other end of the tube was prescribed only with the axial constraint to represent a repeating section. These boundary conditions are appropriate to calculate the blade deflection relative to the base deflections of the tube cross-section.

7.3.1 Blade and Tube Thickness Estimation Procedure

The optimal blade and tube thickness estimations were determined from several runs of the simplified shell models. The following steps describe the procedure followed for the tube and blade thickness estimations. The deflection criteria used in the following procedures were based on the gap leakage limitations and were prescribed by Percheron Power.

For tube thickness estimation:

1. A simplified shell model with constant 1" thick blades and an arbitrary thick tube was constructed and the model was solved for the loads and boundary conditions described earlier to predict the deflections and stresses.
2. Keeping the blade thickness constant, the tube thickness was varied until it behaved similar to a rigid tube and did not influence the blade deflections (i.e., the tube thickness with radial blade deflections that fall within 0.5 mm of the rigid tube solution).
3. The maximum blade deflections in axial and radial directions and maximum principal stresses were tracked in these iterative solutions and the final tube thickness was selected from the solution with axial and radial deflections within 0.5 mm of the rigid tube solution.

Figure 15shows the results from the HBE tube thickness analysis following the described procedure. In this figure, the radial blade deflections (which may increase gap leakage) from all the iterations are well within 0.5 mm of the rigid tube solutions and hence the radial deflection was not the governing factor for the tube thickness selection. The axial deflections vary significantly with blade thickness, and the curve intersects the 0.5 mm offset rigid tube solution when the blade thickness is about 31 mm.

1. For the blade thickness estimation, the tube thickness determined earlier was kept constant and the blade thickness was varied until the blade deflections satisfied the deflection limit criteria of 5 mm axial and 0.5 mm radial deflections.
2. Additionally, the stresses must be less than the composite design strength.

Figure 16 shows the results from the HBE blade thickness analysis. In this figure, the radial blade deflections from all the iterations were again within 0.5 mm, hence radial deflection was not the governing factor for the blade thickness selection. The axial deflections vary significantly with blade thickness and the curve intersects the 5 mm offset line when the thickness is about 24.5 mm. Hence for the HBE design, a tube thickness of 31 mm and a blade thickness of 25 mm were considered appropriate.

7.4 Prototype-Scale Shell Models

Once the blade and tube thickness were established, the full models with shell elements were constructed to estimate the design-specific material requirement, deflections, and stresses. Figure 17a shows the full HBE shell model with the determined blade and tube thicknesses. The full models were built with the same blade and shell materials properties as the single-flight shell models, i.e., quasi-isotopic layup properties for the blades and Ershigs 55° helical wound pressure pipe composite properties for the tube. In the full models, the pressures on the blade were applied assuming the water level at the top of the tube and 25° inclination of the tube, and following the "ρgh" variation illustrated in Figure 14. Figure 17b presents the horizontal displacements (x-direction in the local coordinate system "CSYS-11" shown in Figure 17) of the turbine. The maximum horizontal deflection of 6.9 mm occurred at the blade ends. The blade flights in these full models were also disconnected at 180° flights.

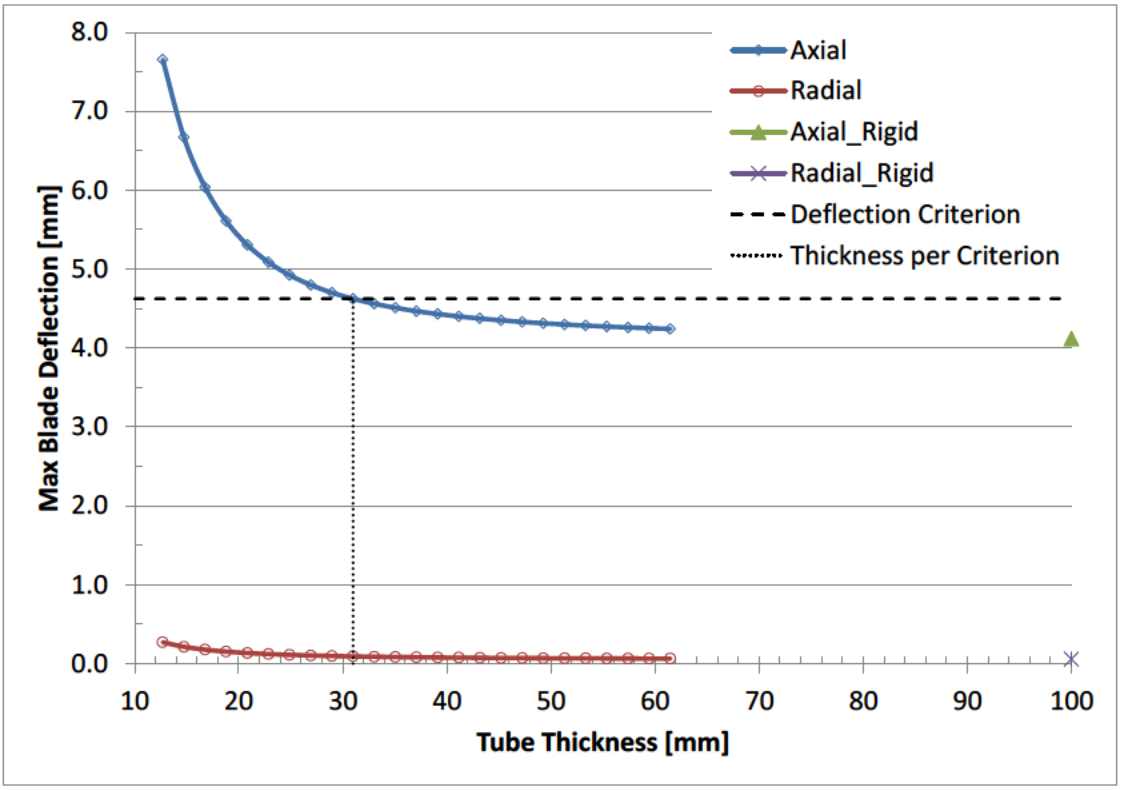

Figure 15. Plot illustrating tube thickness estimation for the HBE design.

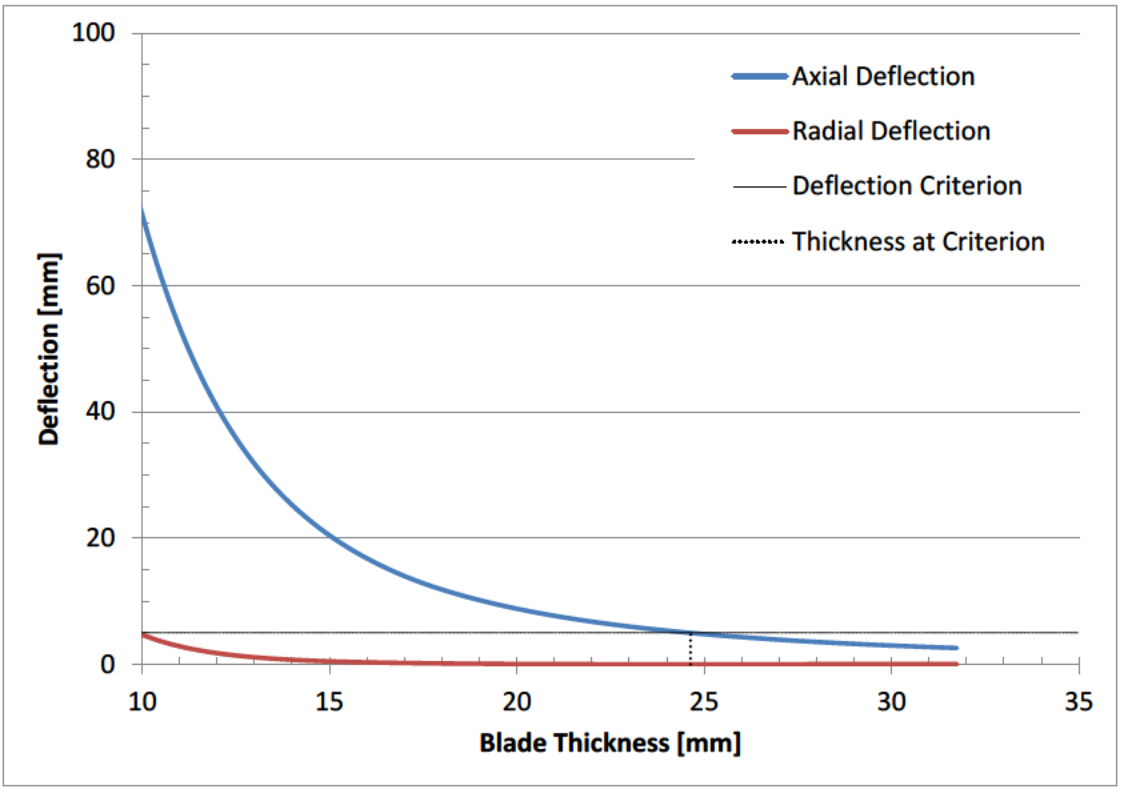

Figure 16. Plot illustrating blade thickness estimation for the HBE design.

[redacted]

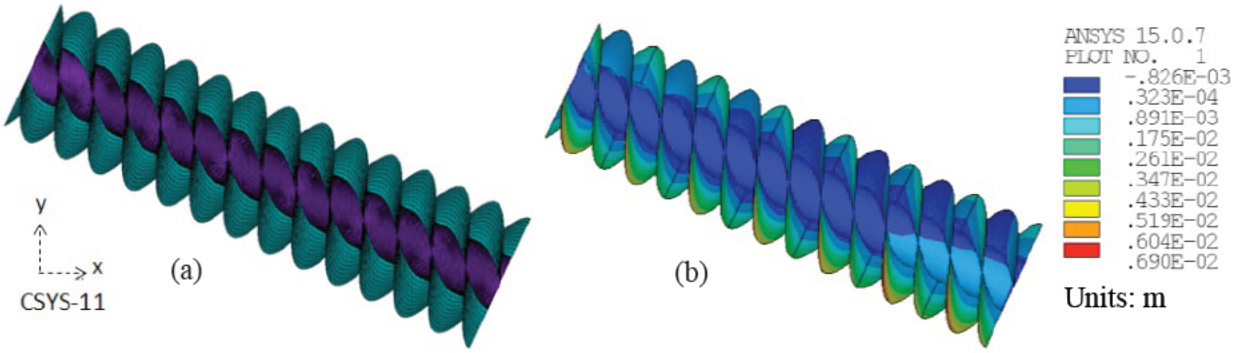

Figure 17. Full model of the HBE design with shell elements (a) and horizontal deformation results (b).

Table 6 presents a summary of the blade and tube thickness estimations from the iterative analysis of the single-flight shell models. The results show that the HBV design required thinner blades and tube. The table also presents the required composite mass from the analysis of the full-scale shell models for each of the four designs considered. From the turbine mass estimates it was evident that the best-volume designs required significantly less composite material, and within the best-volume designs the helicoid profiles required the least amount of composite material. Further, the SBE design required the greatest amount of composite material for turbines designed with the same length and outer diameter.

Table 6. Summary of the tube and blade thickness material requirements.

Model	Tube Thickness[1] (mm)	Blade Thickness[2] (mm)	Tube Mass[4] (kg)	Blade Mass[3,5] (kg)	Total Composite Mass (kg)
HBE	31	24.6	984	1972	2956
HBV	25	18.0	991	779	1770
SBE	31	28.7	984	2758	3742
SBV	31	20.6	1158	1133	2291

NOTES:

1. Tube thickness selection criterion: less than 0.5 mm (axial and radial) deviation from the rigid tube behavior (whichever requires thicker tube).
2. Blade thickness selection criterion: deflections less than 5 mm axial and 0.5 mm radial (whichever requires thicker blade).
3. Four blades were modeled in all the four cases.
4. Tube material based on 42% E-glass by volume (estimate from Ershigs® Data), $\rho = 1.75$ kg/m^3.
5. Blade material based on ~60% E-glass by volume (Quasi-Isotropic layup), $\rho = 1.98$ kg/m^3.

7.5 FEA Models for Blade Root Configuration

Cantilever beam models were developed to study the effect of root and loading configuration on the stresses near the root. These models were built with two-dimensional plane strain elements similar to the composite property validation prototype shown in Figure 9. The initial designs considered a T-type root configuration as shown in Figure 18 (left). While such a configuration may take load in any direction, manufacturing such blades may need complex mold designs and, moreover, the blades are expected to have dominant unidirectional loading that may change periodically rather than a completely reversing load. Hence, the blade root configuration resembling an L-type root as shown in Figure 18 (right) was considered. In these models the nodes along the base were supported with contacts and the nodes along the embedded stainless steel threaded plate location (shown in Figure 9) were fixed in the horizontal and vertical directions to represent a bolted constraint. Structural analysis of the two joint types under the same loading conditions gave similar stress range for both configurations. Because the L type

configuration may simplify the blade mold designs and reduce the manufacturing time and weight, this configuration was recommended for prototype root design.

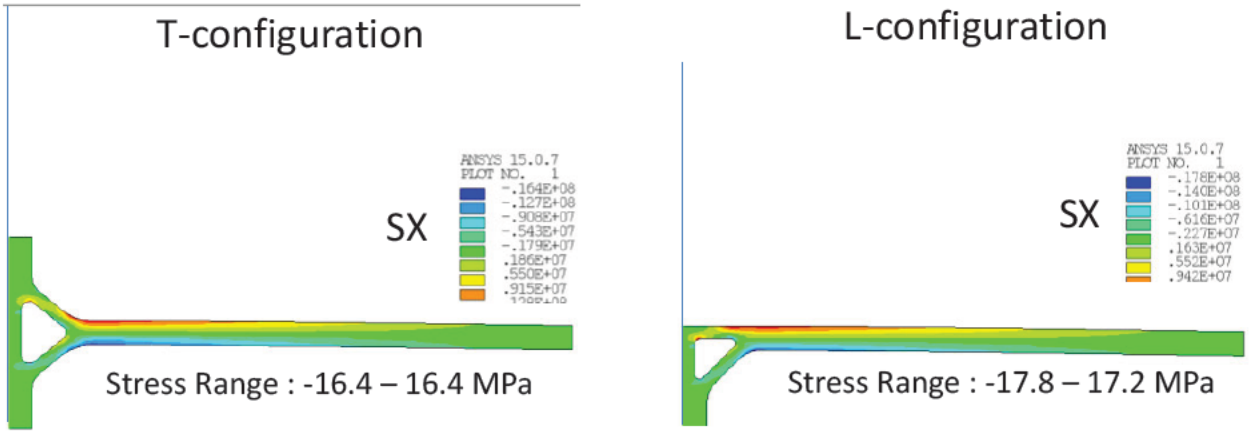

Figure 18. T and L type root configurations with top and bottom layer stresses under the same load.

In the L configuration the stresses in the blade were found to vary based on the direction of loading and the anchor bolt location. Three different loading and anchoring conditions shown in Figure 19 (left) were studied. Results indicated that the configuration in Figure 19c, with bottom side loading and anchor bolt away from the web (at the mid-span of the base), may result in lower stresses (longitudinal tensile and compressive, transverse tensile and compressive, in-plane shear) and could be a preferred configuration. The configuration in Figure 19b produced the largest stresses in all the directions.

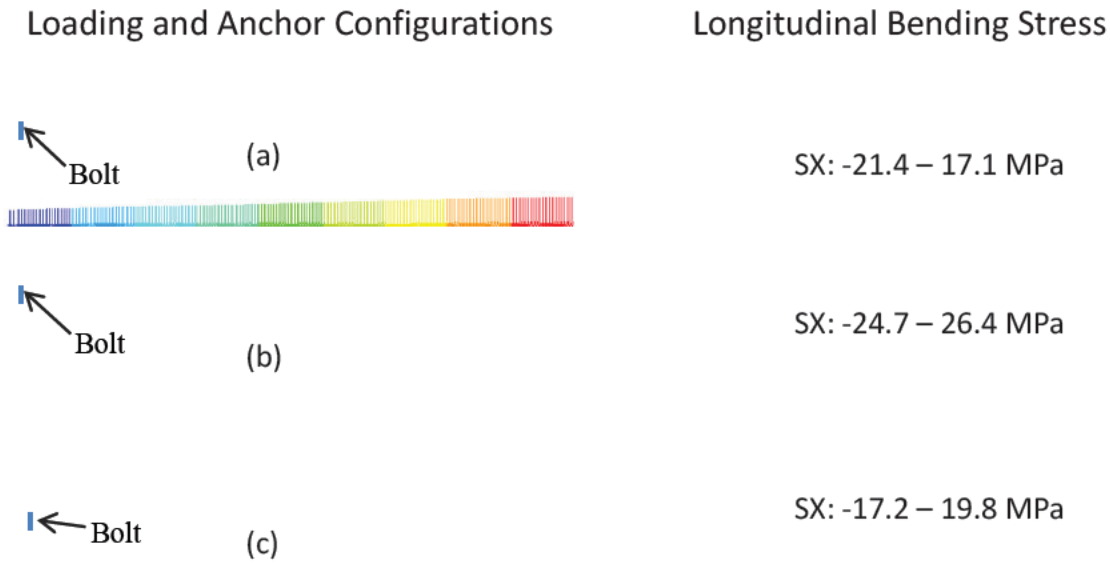

Figure 19. Blade root and loading configurations

7.6 Cyclic Loading Evaluations

Analysis was conducted to verify the occurrence of load reversal on the blades that may enhance fatigue failure probability. The prototype HBE model shown in Figure 11 was used for this study. A series of blade loading pressure profiles that produced high and low torques in the CFD analyses were mapped

onto structural FEA model and analyzed for stresses in the blades. The blade surface and root stress results were checked at a few critical sections, such as the turbine entry and exit locations and the turbine mid-sections. However, the stress variations did not indicate any stress reversals from tension to compression.

8.0 Conclusions and Recommendations

PNNL provided technical assistance to Percheron Power under DOE's SBV pilot program to develop a low-cost, light-weight glass-fiber composite AHS turbine for extracting renewable hydropower from low-head water sources. The assistance was mainly provided through state-of-the-art computational modeling and experimental support of a physical model. Advanced CFD analysis integrated with modern FEA was used to analyze various turbine designs and later to select an optimal design for prototype development and future water testing by Percheron Power. PNNL supercomputing capabilities were used to simulate the dynamic performance of the turbines with CFD analysis.

The CFD analyses simulated the operating performance of AHS turbines of different designs. Results from the bench-scale CFD models were in good agreement with the experiments conducted by Percheron Power. The performance of four different optimized AHS turbine designs was predicted for prototype-scale turbines of 2 m diameter and 7.2 m length. This study shows that the best-volume designs produced higher torques under a given head as expected. However, this study did not predict higher torque with the strake-profiled blades which was the potential as yet untested advantage of the strake blade. The simulations showed that over-filled conditions for all designs may result in higher sloshing during operation, which may be undesirable from loading and operational perspectives. Results from the controlled speed (lower RPM) study indicated higher torque and turbine efficiency.

PNNL analyzed the blade manufacturer's (HRA Inc.) composite laminates and recommended quasi-isotropic [0/+45/-45/90] layup designs for final application. The composite properties estimated using classical lamination theory were in good agreement with those calculated based on the deflection of HRA Inc.'s cantilever beam test with a [0/+45/-45] layup. The materials properties used in all the FEA models were based on the recommended quasi-isotropic [0/+45/-45/90] layup. The structural FEA analyzed the prototype designs for stresses and deflections by mapping the pressures from the CFD analysis. The results from the models with the prototype geometry indicated that the composite turbine geometry based on established steel turbine technology may result in over-designs that enable further optimization. Single-flight (360°) shell element models were developed to expedite the process of design optimization. Procedures were established to determine the tube and blade thickness for different designs based on deflection criteria. These provided the basis for selecting a structurally robust and cost-effective design. The required composite tube and blade thicknesses for four different AHS turbine designs were estimated based on single-flight models and were later used in the full-scale shell models to estimate design-specific material requirements. The models of the prototype-scale turbine indicate that the HBV design requires the least material and could potentially be the most cost-effective for initial prototype fabrication and further testing by Percheron Power.

In addition to the design selection, questions related to the blade root configuration, anchoring requirements (bolt loads and spacing), and the connection between the modular blade flights were addressed during the project. The turbine engineering design correlations and tools that were developed in Mathcad and Excel during the course of the project were transferred to Percheron Power for future usage. The following list presents the additional considerations and recommendations for future work.

- The results from the CFD simulations with four-bladed AHS turbines did not predict the expected performance gain with strake-profiled blades, potentially because of the overfill conditions

considered in the simulations. The bench-scale tests with strake-profiled blades may confirm this outcome and provide additional insights into this behavior.

- Future modeling and testing may consider the effect of the number of blades on the helicoid- and strake-profiled AHS turbine performance, the impact of the shape of the inlet and outlet blades on efficiency, noise performance of the turbines.
- The results from the FEA indicated that overall deflections (tube, blade, tube + blades) rather than stresses could be the limiting criteria for the composite AHS design because the predicted stresses are well within the limits for composite design strength.
- Assuming Percheron Power moves forward and fabricates prototypes of one or more optimized composite AHS designs, it would be very beneficial to compare the results of the planned water-testing of the prototypes at UWRL with the PNNL performance predictions.

9.0 References

1. Rorres C. 2000. The turn of the screw: Optimal design of an Archimedes screw. *Journal of Hydraulic Engineering* 126: 72–80.

2. Nuernbergk DM and Rorres C. 2013. An Analytical Model for the Water Inflow of an Archimedes Screw used in Hydropower Generation. *Journal of Hydraulic Engineering* 139: 213–220

3. U.S Patent no. 61/704,753.

4. Siemens Product Lifecycle Management Software Inc. 2016. STAR-CCM+ User Guide. Plano, Texas.

5. ANSYS, Inc. 2013. ANSYS® 15.0 documentation, Canonsburg, Pennsylvania.

6. SAERTEX USA, LLC. 2016. SAERTEX® SAP-MATERIAL-NO.30000383 Datasheet. SAERTEX USA, Huntersville, North Carolina.

7. Rhino Linings. 2009. Rhino™ 1401-21 / 4101-21 epoxy system for infusion Data Sheet. Rhino Linings Corporation, San Diego, California.

8. Personal communication with Ershigs Inc., Bellingham, Washington.

Distribution

No. of Copies

Name
Organization
Address
City, State and ZIP Code

Organization
Address
City, State and ZIP Code
Name
Name
Name
Name
Name (#)

Name
Organization
Address
City, State and ZIP Code

No. of Copies

 # Foreign Distribution

Name
Organization
Address
Address line 2
COUNTRY

Local Distribution
Pacific Northwest National Laboratory

Name	Mailstop
Name	Mailstop
Name	Mailstop
Name	Mailstop
Name	(PDF)

Pacific Northwest
NATIONAL LABORATORY

Proudly Operated by **Battelle** *Since 1965*

U.S. DEPARTMENT OF
ENERGY

902 Battelle Boulevard
P.O. Box 999
Richland, WA 99352
1-888-375-PNNL (7665)

www.pnnl.gov